

73-151

SEARCH ROUT

Sept. 26, 1967

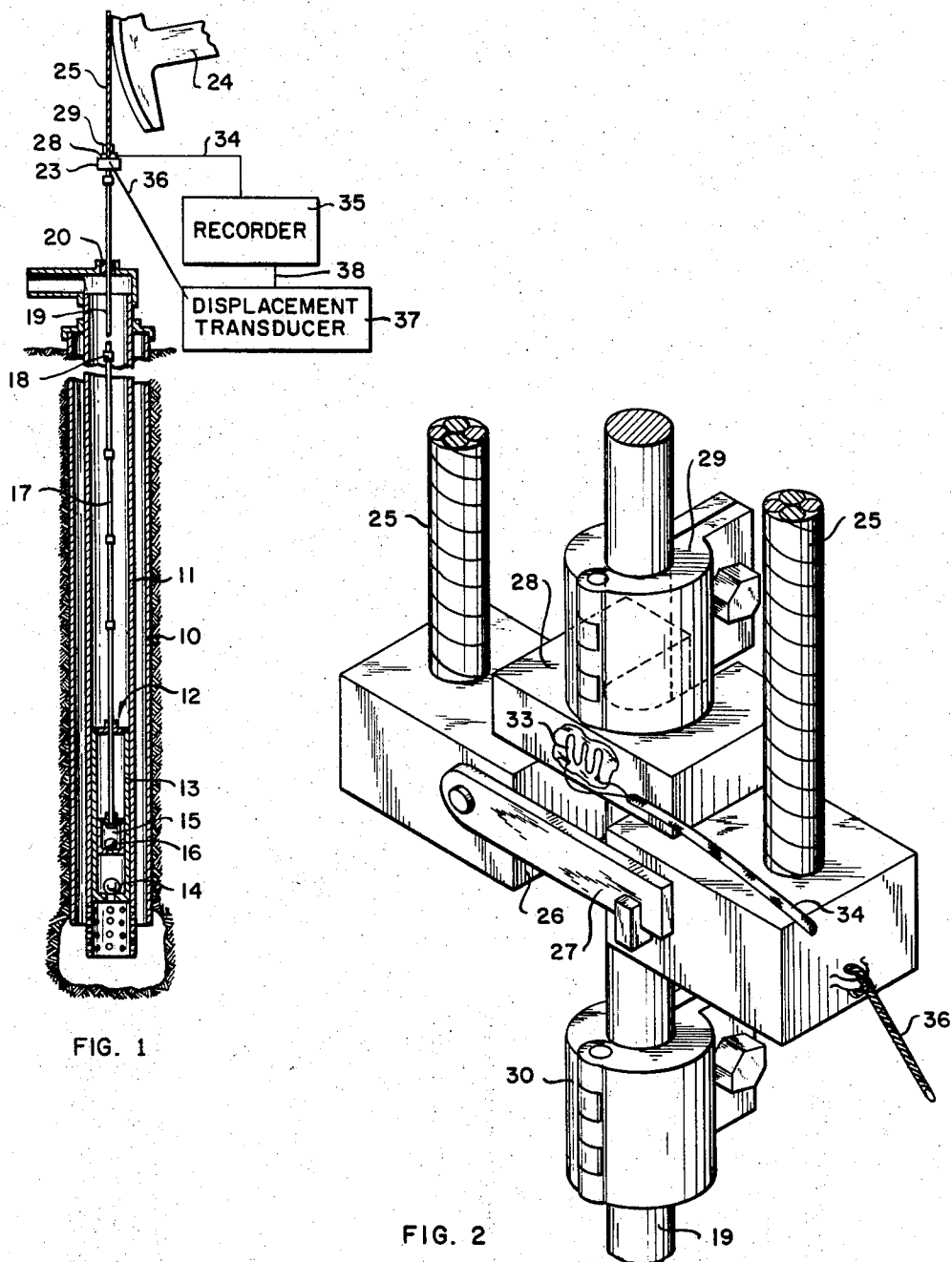
S. G. GIBBS

3,343,409

METHOD OF DETERMINING SUCKER ROD PUMP PERFORMANCE

Filed Oct. 21, 1966

3 Sheets-Sheet 1



INVENTOR:

SAM G. GIBBS

BY: *Donald J. McInroe*

HIS ATTORNEY

Sept. 26, 1967

S. G. GIBBS

3,343,409

METHOD OF DETERMINING SUCKER ROD PUMP PERFORMANCE

Filed Oct. 21, 1966

3 Sheets-Sheet 2

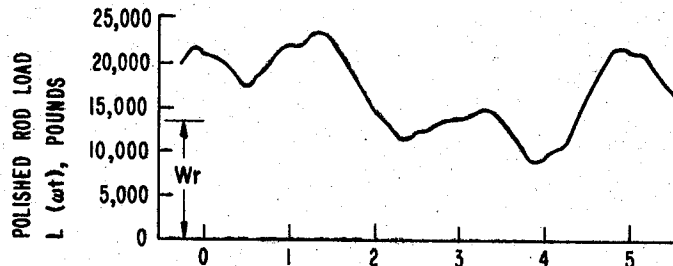


FIG. 3

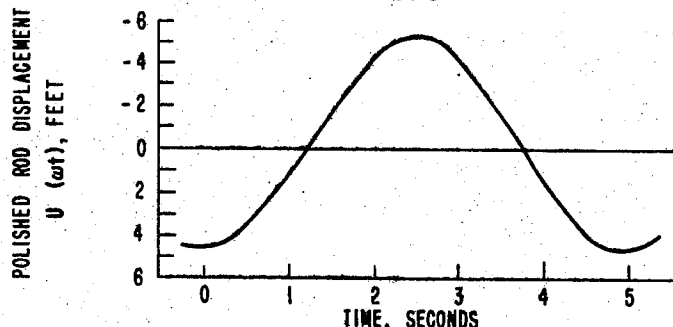


FIG. 4

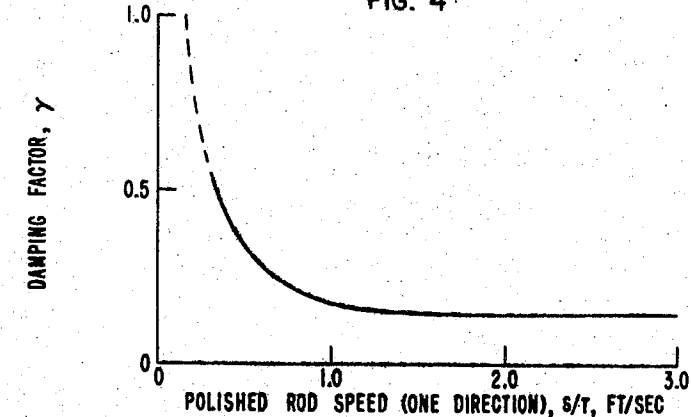


FIG. 5

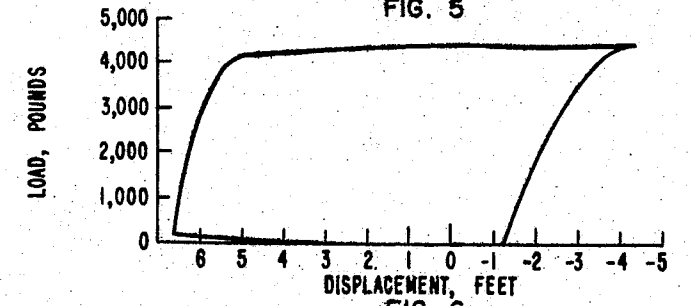


FIG. 6

INVENTOR:

SAM G. GIBBS

BY:

Oswald H. Milmore

HIS ATTORNEY

Sept. 26, 1967

S. G. GIBBS

3,343,409

METHOD OF DETERMINING SUCKER ROD PUMP PERFORMANCE

Filed Oct. 21, 1966

3 Sheets-Sheet 3

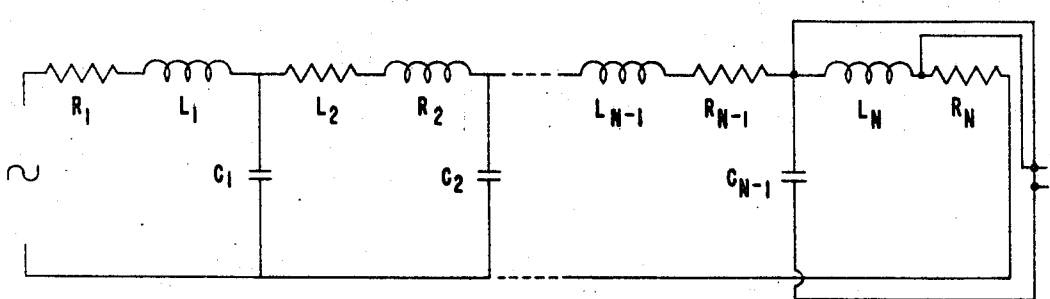


FIG. 7

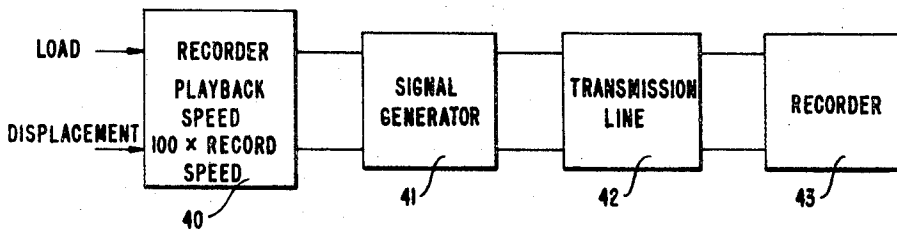


FIG. 8

INVENTOR:
SAM G. GIBBS

United States Patent Office

3,343,409

Patented Sept. 26, 1967

1

3,343,409

METHOD OF DETERMINING SUCKER ROD PUMP PERFORMANCE

Sam G. Gibbs, Houston, Tex., assignor to Shell Oil Company, New York, N.Y., a corporation of Delaware
Filed Oct. 21, 1966, Ser. No. 596,371
3 Claims. (Cl. 73—151)

ABSTRACT OF THE DISCLOSURE

A process for determining the downhole performance of a pumping oil well by measuring data at the surface. The size, length and weight of the sucker rod string are measured and the load and displacement of the polish rod as functions of time are recorded. From the above data it is possible to construct a load versus displacement curve for the sucker rod string at any selected depth in the well.

This application is a continuation-in-part of application Ser. No. 354,236, filed March 24, 1964, now abandoned.

This invention relates to a method for determining the performance characteristics of a pumping well. More particularly, the invention is directed to a method of determining downhole conditions of a pumping well from data which are received, measured and manipulated at the surface of the well. The invention has specific application to the analysis of pumping problems in the operation of sucker rod pumping systems.

For pumping deep wells, such as oil wells, a common practice is to employ a series of interconnected rods for coupling an actuating device at the surface with a pump at the bottom of the well. This series of rods, generally referred to as the rod string or sucker rod, has the uppermost rod extending up through the well casinghead for connection with an actuating device, such as a pump jack of the walking beam type, through a coupling device generally referred to as the rod hanger. The well casinghead includes means for permitting sliding action of the uppermost rod which is generally referred to as the "polished rod."

In deep wells the long sucker rod has considerable stretch, distributed mass, etc., and motion at the pump end may be radically different from that imparted at the upper end. Through the years, the polished rod dynamometer has provided the principal means for analyzing the performance of rod pumped wells. The dynamometer is an instrument which records a curve, usually called a card, of polished rod load versus displacement. The shape of this curve reflects the conditions which prevail downhole in the well. Hopefully the downhole conditions can be deduced by visual inspection of the polished rod card. Owing to the diversity of card shapes, however, it is frequently impossible to make a diagnosis of downhole conditions solely on the basis of visual interpretation. In addition to being highly dependent on the skill of the dynamometer analyst, the method of visual interpretation only provides downhole data which are qualitative in nature. As a result it is frequently necessary to use complicated apparatus and procedures to directly take downhole measurements in order to accurately determine the performance characteristics at various depth levels within the well.

Broadly, the present invention provides a system for economically preparing downhole dynagraph cards at all depth levels, including the pump, from data which are measured uphole at the polished rod. As a result, the system provides a rational, quantitative method for determining downhole conditions which is independent of the skill and experience of the analyst. It is no longer necessary to guess at downhole operating conditions on the

2

basis of recordings taken several thousands of feet above at the polished rod, or to undertake the expensive and time consuming operation of running an instrument to the bottom of the well in order to measure such conditions. By use of the method, it is possible to directly determine the subsurface conditions from data received at the top of the well.

The invention will now be described with reference to the accompanying drawings wherein:

FIGURE 1 is a schematic diagram partially in longitudinal section, showing the general arrangement of apparatus in a system in accordance with the invention;

FIGURE 2 is an enlarged side elevation showing a portion of the apparatus at the rod hanger;

FIGURE 3 is a graphical illustration of polished rod load versus time;

FIGURE 4 is a graphical illustration of polished rod displacement versus time;

FIGURE 5 is a curve illustrating the relation between polished rod speed and a damping factor;

FIGURE 6 is a pump dynagraph card constructed in accordance with the present invention;

FIGURE 7 is a circuit diagram of an equivalent transmission line corresponding to the sucker rod string shown in FIGURE 1; and,

FIGURE 8 is an analog computer utilizing the transmission line of FIGURE 7 for providing a dynagraph card at any selected depth in the well.

Referring to FIGURE 1, there is shown a well having the usual well casing 10 extending from the surface to the bottom thereof. Positioned within the well casing 10 is a production tubing 11 having a pump 12 located at the lower end. The pump barrel 13 contains a standing valve 14 and a plunger or piston 15 which in turn contains a traveling valve 16. The plunger 15 is actuated by a jointed sucker rod 17 that extends from the piston 15 up through the production tubing to the surface and is connected at its upper end by a coupling 18 to a polished rod 19 which extends through a packing joint 20 in the wellhead.

As best shown in FIGURE 2, the upper end of the polished rod 19 is connected to a hanger bar 23 suspended from a pumping beam 24 by two wire cables 25. The hanger bar 23 has a U-shaped slot 26 for receiving the polished rod 19. A latching gate 27 prevents the polished rod from moving out of the slot 26. A U-shaped platform 28 is held in place on top of the hanger bar 23 by means of a clamp 29. A similar clamp 30 is located below the hanger bar 23. A strain-gauge load cell 33, described in greater detail hereafter, is shown bonded to the platform 28. An electrical cable 34 leads from the load cell 33 to a recorder 35, and a taut wire line 36 leads from the hanger bar 23 to a displacement transducer 37 (see FIGURE 1). The displacement transducer 37 is also connected to the recorder 35 by the electrical lead 38.

The strain-gauge load cell 33 is a conventional device and operates in a manner well known to those in the art. A particularly suitable load cell is the model 1011 manufactured by Lockheed Electronics Company, Los Angeles, California. When the platform 28 is loaded, it becomes shorter and fatter due to a combination of axial and transverse strain. Since the wire of the strain-gauge 28 is bonded to the platform 28, it is also strained in a similar fashion. As a result, a current passed through the strain-gauge wire now has a larger cross section of wire in which to flow, and the wire is said to have less resistance. As the hanger bar 23 moves up and down, an electrical signal which relates strain-gauge resistance to polished rod load is transmitted from the load cell 33 to the recorder 35 via the electrical cable 34.

The displacement transducer 37 is a conventional unit such as the Model WR8-150-A also manufactured by

3

Lockheed Electronics Company. The displacement transducer unit 37 is a cable-and-reel driven, infinite resolution potentiometer that is equipped with a constant tension ("negator" spring driven) rewind assembly. As the hanger bar 23 moves up and down, the taut wire line 36 actuates the reel driven potentiometer and a varying voltage signal is produced. This signal, which relates voltage to polished rod displacement, is also transmitted to the recorder 35 via the electrical lead 38.

The recorder 35 is a conventional instrument such as the Model G-22 Dual Channel Recorder manufactured by Varian Associates, Inc. The recorder 35 is provided with a high torque motor which drives a strip chart at the rate of 60 inches per minute. Data from the strain-gauge load cell 33 and the displacement transducer 37 are simultaneously and independently recorded on the common chart to produce curves as shown in FIGURES 3 and 4. FIGURE 3 shows a typical curve of polished rod load versus time and FIGURE 4 shows a curve illustrating polished rod displacement versus time.

The key part in the analysis of the pumping system performance is the method for deciphering the force data which are measured at the polished rod. This interpretive process is based on a boundary-value problem comprising a differential equation and a set of boundary conditions.

The sucker rod can be thought of as a transmission or communication line, the behavior of which is described by the viscously damped wave equation:

$$\frac{\partial^2 u(x,t)}{\partial t^2} = a^2 \frac{\partial^2 u(x,t)}{\partial x^2} - c \frac{\partial u(x,t)}{\partial t} \quad (1)$$

where:

a =velocity of sound in steel in feet/second;

c =damping coefficient, 1/second;

t =time in seconds;

x =distance of a point on the unrestrained rod measured from the polished rod in feet; and,

$u(x,t)$ =displacement from the equilibrium position of the sucker rod in feet.

In reality, damping in a sucker rod system is a complicated mixture of many effects. The viscous damping law postulated in Equation 1 lumps all of these damping effects into an equivalent viscous damping term. The criterion of equivalence is that the equivalent force removes from the system as much energy per cycle as that removed by the real damping forces.

In keeping with this viscous damping postulate, some field damping measurements have been made. FIGURE 5 shows an idealization of these measurements phrased in terms of a dimensionless damping constant, γ . The damping coefficient, c , used in our analysis can be determined from FIGURE 5 and the relation:

$$c = \frac{\pi a \gamma}{2L} \quad (2)$$

where:

γ =dimensionless damping factor; and,

$L=x_1+x_2+\dots+x_m$ =combined length of rods (depth of pump), in feet.

An alternate way of estimating the damping coefficient is by means of Equation 2 and the relation:

$$\gamma = \frac{4.42 \times 10^{-2} L (PRhp - Hhp) T^2}{(A_1 x_1 + A_2 x_2 + \dots + A_m x_m) S^2} \quad (3)$$

where:

$PRhp$ =polished rod horsepower, in horsepower;

Hhp =pump hydraulic horsepower, in horsepower;

T =period of pumping cycle, in seconds;

A_1, A_2, \dots, A_m =area of each rod size in the combination string in square inches;

4

x_1, x_2, \dots, x_m =length of each rod interval in the combination string in feet; and,
 S =polished rod stroke, in feet.

Equation 3 is derived by assuming that the viscous damping losses occur as though the integrated average velocity of the sucker rod were equivalent to the root mean square velocity of the polished rod in simple harmonic motion. Either of these two methods for estimating the damping factor may prove suitable. Investigations have shown that

10 the wave Equation 1 including the viscous damping approximation, gives good practical results when applied to sucker rod problems.

Information regarding downhole operating conditions is transmitted through the sucker rod in the form of strain

15 waves which travel at about 16,000 feet per second. This information is monitored at the polished rod, preferably in the form of curves of polished rod load and displacement versus time as shown respectively in FIGURES 3 and 4. The boundary conditions are then formulated with

20 this measured information or data. Because Equation 1 contains no gravity term, the rod weight must be deducted from the polished rod load. This yields a dynamic load-time curve which, together with the displacement time

25 curve, constitutes the boundary condition data required for a steady-state solution. The boundary conditions are formulated analytically by approximating these curves with a truncated Fourier series of the type:

$$30 D(\omega t) = L(\omega t) - W_r = \frac{\sigma_o}{2} + \sum_{n=1}^{\infty} \sigma_n \cos n\omega t + \tau_n \sin n\omega t \quad (4)$$

and

$$35 U(\omega t) = \frac{\nu_o}{2} + \sum_{n=1}^{\infty} \nu_n \cos n\omega t + \delta_n \sin n\omega t \quad (5)$$

where:

40 ω =angular velocity in radians per second;
 $D(\omega t)$ =dynamic polished rod load function in pounds;
 $L(\omega t)$ =total polished rod load function in pounds;
 W_r =rod weight in fluid in pounds; and,
 $U(\omega t)$ =polished rod displacement function in feet.

45 These are the force-time and displacement-time functions.

The Fourier coefficients σ , τ , ν and δ shown above are evaluated from the measured data by use of harmonic analysis as set out below. To apply the method, it is necessary to evaluate Fourier coefficients associated with 50 functions defined only in graphical form. Since no explicit equations are available for these functions, evaluation of the coefficients by the classical method of integration is not possible. The following is a simple numerical procedure for approximating these coefficients:

55 Consider the dynamic load-time function $D(\omega t)$. This function can be approximated by a truncated Fourier series, provided that the following integrals are used to evaluate the coefficients:

$$60 \sigma_n = \frac{\omega}{\pi} \int_0^{2\pi} D(\omega t) \cos n\omega t dt, \quad n=0, 1, 2, \dots, \bar{n}$$

$$\tau_n = \frac{\omega}{\pi} \int_0^{2\pi} D(\omega t) \sin n\omega t dt, \quad n=1, 2, \dots, \bar{n}$$

65 These integrals can be approximated as follows. Let $\theta=\omega t$, and obtain, for the σ_n ,

$$1\sigma_n = \frac{1}{\pi} \int_0^{2\pi} D(\theta) \cos n\theta d\theta, \quad n=0, 1, 2, \dots, \bar{n}$$

70 For the numerical integration, consider θ as a discrete variable

$$\theta = \frac{2\pi p}{K}, \quad p=0, 1, 2, \dots, K$$

Adopt the shorter notation

$$\frac{D \cdot 2\pi p}{K} = D_p$$

etc., and use a trapezoid rule to write

$$\begin{aligned} \sigma_n &\approx \frac{1}{\pi} \left[\frac{D_0 \cos \left[\frac{2n\pi \cdot 0}{K} \right] + D_1 \cos \left[\frac{2n\pi \cdot 1}{K} \right]}{2} + \right. \\ &\quad \frac{D_1 \cos \left[\frac{2n\pi \cdot 1}{K} \right] + D_2 \cos \left[\frac{2n\pi \cdot 2}{K} \right]}{2} + \dots + \\ &\quad \left. \frac{D_{K-1} \cos \left[\frac{2n\pi(K-1)}{K} \right] + D_K \cos(2n\pi)}{2} \right] \frac{2\pi}{K} \end{aligned}$$

Collecting like terms we have

$$\begin{aligned} \sigma_n &\approx \frac{2}{K} \left[\frac{D_0 \cos 0}{2} + D_1 \cos \left[\frac{2n\pi \cdot 1}{K} \right] + D_2 \cos \left[\frac{2n\pi \cdot 2}{K} \right] + \right. \\ &\quad \left. \dots + \frac{D_K \cos(2n\pi)}{2} \right]. \end{aligned}$$

For a periodic function, $D_0 = D_K$. Also, $\cos 0 = \cos 2n\pi$; hence,

$$\sigma_n \approx \frac{2}{K} \sum_{p=1}^K D_p \cos \frac{2n\pi p}{K}, \quad n = 0, 1, \dots, \bar{n}$$

The other Fourier coefficients are obtained in like fashion. Thus,

$$\tau_n \approx \frac{2}{K} \sum_{p=1}^K D_p \sin \left[\frac{2n\pi p}{K} \right], \quad n = 1, 2, 3, \dots, \bar{n}$$

$$\nu_n \approx \frac{2}{K} \sum_{p=1}^K U_p \cos \left[\frac{2n\pi p}{K_1} \right], \quad n = 0, 1, 2, \dots, \bar{n}$$

$$\delta_n \approx \frac{2}{K} \sum_{p=1}^K U_p \sin \left[\frac{2n\pi p}{K_1} \right], \quad n = 1, 2, \dots, \bar{n}$$

The accuracy of the numerical integration described above depends on the number of ordinates that are taken. Determination of the optimum number of ordinates is difficult, but a K of 75 will probably suffice for the calculation of the force coefficients σ_n and τ_n . Fewer ordinates are required for the displacement coefficients ν_n and δ_n , because the displacement function $U(\omega t)$ is quite smooth. Perhaps a K_1 of 35 is sufficient.

The smooth nature of the displacement function also permits the use of fewer displacement coefficients. Perhaps a maximum of four coefficients is required; therefore, the remaining coefficients $\nu_5, \nu_6, \dots, \nu_n$ and $\delta_5, \delta_6, \dots, \delta_n$ may be neglected.

To solve the problem set forth by Equations 1, 2 and 3, let $z(x, t)$ be a complex variable. The wave Equation 1 then becomes, in complex form,

$$\frac{\partial^2 z(x, t)}{\partial t^2} = a^2 \frac{\partial^2 z(x, t)}{\partial x^2} - c \frac{\partial z(x, t)}{\partial t} \quad (6)$$

Employing separation of variables, we seek product solutions of the form

$$z(x, t) = X(x)T(t)$$

where $X(x)$ and $T(t)$ are, respectively, functions of x and t alone. Differentiation and substitution into Equation 6 yields

$$\frac{T''(t)}{a^2 T(t)} + \frac{c T'(t)}{a^2 T(t)} = \frac{X''(x)}{X(x)}$$

Each side of the above equation contains only one of the independent variables; hence

$$\frac{T''(t)}{a^2 T(t)} + \frac{c T'(t)}{a^2 T(t)} = \frac{X''(x)}{X(x)} = -\lambda_n^2$$

where λ_n is a separation constant. This separation process splits the partial differential equation into two ordinary differential equations

$$T''(t) + c T'(t) - \lambda_n^2 a^2 T(t) = 0 \quad (7)$$

and

$$X''(x) + \lambda_n^2 X(x) = 0 \quad (8)$$

Products of solutions to Equations 7 and 8 satisfy Equation 6. Anticipating Fourier series expansions in t , we seek periodic solutions to Equation 7 of the type

$$T(t) : e^{in\omega t}$$

Differentiation and substitution into Equation 7 yields

$$-n^2 \omega^2 e^{in\omega t} + i c n \omega e^{in\omega t} + \lambda_n^2 a^2 e^{in\omega t} = 0$$

Since $e^{in\omega t} \neq 0$, then

$$\lambda_n^2 = \frac{n^2 \omega^2 - i c n \omega}{a^2}$$

Using methods in complex variables, we find

$$\lambda = \pm \sqrt{\frac{-n\omega}{a\sqrt{2}}} \sqrt{1 + \sqrt{1 + \left[\frac{c}{n\omega} \right]^2}} +$$

$$\frac{i n \omega}{a \sqrt{2}} \sqrt{-1 + \sqrt{1 + \left[\frac{c}{n\omega} \right]^2}}$$

Let us choose the positive root, and define

$$\lambda_n = -\alpha_n + i\beta_n \quad (9)$$

where

$$\alpha_n = \frac{n\omega}{a\sqrt{2}} \sqrt{1 + \sqrt{1 + \left[\frac{c}{n\omega} \right]^2}} \quad (10)$$

and

$$\beta_n = \frac{n\omega}{a\sqrt{2}} \sqrt{-1 + \sqrt{1 + \left[\frac{c}{n\omega} \right]^2}} \quad (11)$$

Equation 8 is the harmonic equation which is satisfied by linear combinations of

$$X(x) : \sin \lambda_n x, \cos \lambda_n x$$

Special treatment is required for the case when $n=0$. In this instance Equations 7 and 8 reduce to

$$\begin{aligned} T''(t) + c T'(t) &= 0 \\ X''(x) &= 0 \end{aligned}$$

Solutions to these equations which are of interest are

$$\begin{aligned} T(t) &: \xi \\ X(x) &: \eta x, \xi \end{aligned}$$

where ξ, η , and ξ are real constants. This completes the preliminary work. Our choice of product solutions is governed by the boundary conditions. Take

$$z(x, t) = \xi \eta x + \xi \xi + \sum_{n=1}^{\infty} (\Phi_n \sin \lambda_n x + \Theta_n \cos \lambda_n x) e^{in\omega t} \quad (12)$$

where Φ_n and Θ_n are complex constants

$$\begin{aligned} \Phi_n &= -k_n - i\mu_n \\ \Theta_n &= \nu_n - i\delta_n \end{aligned}$$

By the proper choice of these constants, the boundary conditions will be satisfied. As a solution to Equation 1, choose

$$u(x, t) = \operatorname{Re}[z(x, t)] \quad (13)$$

therefore, boundary condition 4 can be satisfied if

$$D(\omega t) = \operatorname{Re} \left[E A \frac{\partial z(0, t)}{\partial x} \right]$$

We have

$$\frac{\partial z(x, t)}{\partial t} = \xi \eta + \sum_{n=1}^{\infty} (\Phi_n \lambda_n \cos \lambda_n x - \Theta_n \lambda_n \sin \lambda_n x) e^{in\omega t}$$

hence,

$$D(\omega t) = EB \left[\xi \eta + \sum_{n=1}^{\infty} (k_n \alpha_n + \mu_n \beta_n) \cos n\omega t + (k_n \beta_n - \mu_n \alpha_n) \sin n\omega t \right] \quad 5$$

It is convenient to define new constants at this point. Take

$$\sigma_n = EA(k_n \alpha_n + \mu_n \beta_n), \quad n=0, 1, 2, \dots \quad (14)$$

$$\tau_n = EA(k_n \beta_n - \mu_n \alpha_n), \quad n=1, 2, \dots \quad (15)$$

$$\sigma_0 = 2EA\xi\eta \quad (16)$$

From Equations 14 and 15, we deduce

$$\kappa_n = \frac{\sigma_n \alpha_n + \tau_n \beta_n}{EA(\alpha_n^2 + \beta_n^2)}, \quad n=1, 2, 3, \dots \quad (17)$$

$$\mu_n = \frac{\sigma_n \beta_n - \tau_n \alpha_n}{EA(\alpha_n^2 + \beta_n^2)}, \quad n=1, 2, 3, \dots \quad (18)$$

In order that boundary Conditions 4 be satisfied, the σ_n and τ_n must be evaluated with the Fourier-Euler integral formulas

$$\sigma_n = \frac{\omega}{\pi} \int_0^{2\pi} D(\omega t) \cos n\omega t dt, \quad n=0, 1, 2, \dots \quad (19)$$

$$\tau_n = \frac{\omega}{\pi} \int_0^{2\pi} D(\omega t) \sin n\omega t dt, \quad n=1, 2, \dots \quad (20)$$

Condition 5 requires that

$$U(\omega t) = \text{Re}[z(0, t)]$$

hence,

$$U(\omega t) = \xi \xi + \sum_{n=1}^{\infty} \nu_n \cos n\omega t + \delta_n \sin n\omega t$$

If

$$\nu_n = \frac{\omega}{\pi} \int_0^{2\pi} U(\omega t) \cos n\omega t dt, \quad n=0, 1, 2, \dots \quad (21)$$

$$\delta_n = \frac{\omega}{\pi} \int_0^{2\pi} U(\omega t) \sin n\omega t dt, \quad n=1, 2, \dots \quad (22)$$

and

$$\nu_0 = 2\xi\eta \quad (23)$$

then Condition 5 will be satisfied. This concludes the procedure for evaluating the separation constants.

The formula for the displacement $u(x, t)$ is determined by using Equation 13 and the complex identities

$$\begin{aligned} \sin \lambda_n x &= -\sin \alpha_n x \cosh \beta_n x + i \cos \alpha_n x \sinh \beta_n x \\ \cos \lambda_n x &= \cos \alpha_n x \cosh \beta_n x + i \sin \alpha_n x \sinh \beta_n x \end{aligned}$$

and

$$e^{in\omega t} = \cos n\omega t + i \sin n\omega t$$

Using these identities, we isolate the real part of $z(x, t)$, obtaining

$$u(x, t) = \frac{\sigma_0}{2EA} x + \frac{\nu_0}{2} + \sum_{n=1}^{\infty} O_n(x) \cos n\omega t + P_n(x) \sin n\omega t \quad (24)$$

where

$$O_n(x) = (\kappa_n \cosh \beta_n x + \delta_n \sinh \beta_n x) \sin \alpha_n x + (\mu_n \sinh \beta_n x + \nu_n \cosh \beta_n x) \cos \alpha_n x \quad (25)$$

and

$$P_n(x) = (\kappa_n \sinh \beta_n x + \delta_n \cosh \beta_n x) \cos \alpha_n x - (\mu_n \cosh \beta_n x + \nu_n \sinh \beta_n x) \sin \alpha_n x \quad (26)$$

The force $F(x, t)$ can be calculated by using Equation 24 and Hooke's law

$$F(x, t) = EA \frac{\partial u(z, t)}{\partial x}$$

We have

$$F(x, t) = EA \left[\frac{\sigma_0}{2EA} + \sum_{n=1}^{\infty} O_n'(x) \cos n\omega t + P_n' \sin n\omega t \right] \quad (27)$$

where

$$O_n'(x) = \left[\frac{\tau_n}{EA} \sinh \beta_n x + (\delta_n \beta_n - \nu_n \alpha_n) \cosh \beta_n x \right] \sin \alpha_n x + \left[\frac{\sigma_n}{EA} \cosh \beta_n x + (\nu_n \beta_n + \delta_n \alpha_n) \sinh \beta_n x \right] \cos \alpha_n x \quad (28)$$

and

$$P_n'(x) = \left[\frac{\tau_n}{EA} \cos \beta_n x + (\delta_n \beta_n - \nu_n \alpha_n) \sinh \beta_n x \right] \cos \alpha_n x - \left[\frac{\sigma_n}{EA} \sinh \beta_n x + \nu_n \beta_n + \delta_n \alpha_n \right] \cosh \beta_n x \quad (29)$$

This completes the formal solution.

In practice, rod strings often involve several rod sizes. This requires that the solution just derived be extended slightly. It is convenient to adopt a more general notation, as follows. Let $A_1, A_2, A_3, \dots, A_m$ be the areas and $x_1, x_2, x_3, \dots, x_m$ be the corresponding lengths of the various rod sections taken in order starting from the surface. Extend the notation for the Fourier coefficients to include two subscripts as ${}^1\sigma_n, {}^1\nu_n, {}^1\delta_n$, where the right subscript denotes the order of the coefficient, as always, and the left subscript denotes the section of the rod string with which the coefficient is associated. The coefficients ${}^1\sigma_n, {}^1\nu_n, {}^1\delta_n$, are understood to pertain to polished rod data (the polished rod is considered as part of the first rod section). Also extend the notation for the functions given in Equations 25, 26, 28, and 29, i.e., ${}^1O_n(x), {}^1P_n(x), {}^jO_n(x)$, and ${}^jP_n(x)$. Here the left subscript denotes that these functions involve the j th set of Fourier coefficients.

For simplicity, consider a two-way taper. The displacement at the bottom of the first section is given by the generalized form of Equation 24 as

$$u(x_1, t) = \frac{{}^1\sigma_0}{2EA_1} x_1 + \frac{{}^1\nu_0}{2} + \sum_{n=1}^{\infty} {}^1O_n(x_1) \cos n\omega t + {}^1P_n(x_1) \sin n\omega t$$

The force in the rod at that point is

$$F(x_1, t) = EA_1 \left[\frac{{}^1\sigma_0}{2EA_1} + \sum_{n=1}^{\infty} {}^1O_n'(x_1) \cos n\omega t + {}^1P_n'(x_1) \sin n\omega t \right] \quad (45)$$

At the junction between the two rod sections, the displacements and forces are continuous. We thus formulate new boundary conditions (parallel to Equations 4 and 5, where x_1 is considered as the new origin) preparatory to computing the displacements and forces in the second rod interval. These new boundary conditions essentially involve a new set of Fourier coefficients. From continuity considerations, the new displacement coefficients become

$${}^2\nu_0 = \frac{{}^1\sigma_0 x_1}{EA_1} + {}^1\nu_0$$

$${}^2\nu_n = {}^1O_n(x_1)$$

$${}^2\delta_n = {}^1P_n(x_1)$$

Similarly, the new force coefficients become

$$\begin{aligned} {}^2\sigma_0 &= {}^1\sigma_0 \\ {}^2\sigma_n &= EA_1 {}^1O_n'(x_1) \\ {}^2\nu_n &= EA_1 {}^1P_n'(x_1) \end{aligned}$$

Finally, the displacement and load at the pump can be computed from

$$u(x_2, t) = \frac{{}^2\sigma_0}{2EA_2} x_2 + \frac{{}^2\nu_0}{2} + \sum_{n=1}^{\infty} {}^2O_n(x_2) \cos n\omega t + {}^2P_n(x_2) \sin n\omega t \quad (70)$$

and

$$F(x_2, t) = EA_2 \left[\frac{2\sigma_0}{2EA_2} + \sum_{n=1}^{\infty} {}_2O'_n(x_2) \cos n\omega t + {}_2P'_n(x_2) \sin n\omega t \right]$$

This procedure suggests recursion formulas for strings with any number of rod sizes. These formulas are

$${}_{j+1}\nu_o = \frac{j\sigma_0 x_j}{EA_j} + \nu_o \quad (30)$$

$${}_{j+1}\nu_n = {}_jO_n(x_j) \quad (31)$$

$${}_{j+1}\delta_n = {}_jP_n(x_j) \quad (32)$$

$${}_{j+1}\sigma_0 = \sigma_0 \quad (33)$$

$${}_{j+1}\sigma_n = EA_j {}_jO'_n(x_j) \quad (34)$$

$${}_{j+1}\tau_n = EA_j {}_jP'_n(x_j) \quad (35)$$

With $j=1, 2, \dots, m-1$, where m is the number of rod sizes comprising the sucker rod string.

The solution to the boundary-value problem given above is fairly lengthy; thus, it is desirable to assemble in one place all of the pertinent formulas. The following is essentially a step-by-step procedure to be followed in performing this analysis:

Step 1. Using the measured data, construct the dynamic load function

$$D(\omega t) = L(\omega t) - W_r \quad (36)$$

Calculate the Fourier coefficients associated with the measured data from

$$\sigma_n = \frac{\omega}{\pi} \int_0^{2\pi} D(\omega t) \cos n\omega t dt, \quad n=0, 1, 2, \dots, \bar{n}$$

$$\tau_n = \int_0^{2\pi} D(\omega t) \sin n\omega t dt, \quad n=1, 2, \dots, \bar{n} \quad (37)$$

$$\nu_n = \frac{\omega}{\pi} \int_0^{2\pi} U(\omega t) \cos n\omega t dt, \quad n=0, 1, 2, \dots, \bar{n}$$

$$\delta_n = \frac{\omega}{\pi} \int_0^{2\pi} U(\omega t) \sin n\omega t dt, \quad n=1, 2, \dots, \bar{n} \quad (45)$$

The polished rod load and displacement functions will be available only in graphical form; therefore, the integrals shown above cannot be evaluated in the classical manner. Many numerical methods, such as harmonic analysis methods, for approximating these integrals are available. A simplified harmonic analysis routine has previously been set out. The number of terms in the truncated Fourier series is determined by \bar{n} . If we increase \bar{n} , the accuracy of the results is increased, but, at the same time, the computation labor is increased. This requires a compromise on the size of \bar{n} . An \bar{n} of, say, 10 will probably suffice in most cases.

Step 2. Estimate the damping coefficient c . Methods for estimating c have been set out, supra. Calculate

$$\omega = \frac{2\pi}{T} \quad (38)$$

$$\alpha_n = \frac{n\omega}{a\sqrt{2}} \sqrt{1 + \sqrt{1 + \frac{c^2}{n\omega}}} \quad (39)$$

$$\beta_n = \frac{n\omega}{a\sqrt{2}} \sqrt{-1 + \sqrt{1 + \frac{c^2}{n\omega}}} \quad (40)$$

$$\kappa_n = \frac{i\sigma_n \alpha_n + i\tau_n \beta_n}{EA_1 (\alpha_n^2 + \beta_n^2)} \quad (41)$$

(40)

$$\mu_n = \frac{i\sigma_n \beta_n - i\tau_n \alpha_n}{EA_1 (\alpha_n^2 + \beta_n^2)} \quad (42)$$

$${}_1O_n(x_1) = ({}_{1\kappa_n} \cosh \beta_n x_1 + {}_{1\delta_n} \sinh \beta_n x_1) \sin \alpha_n x_1 + ({}_{1\mu_n} \sinh \beta_n x_1 + {}_{1\nu_n} \cosh \beta_n x_1) \cos \alpha_n x_1 \quad (43)$$

$${}_1P_n(x_1) = ({}_{1\kappa_n} \sinh \beta_n x_1 + {}_{1\delta_n} \cosh \beta_n x_1) \cos \alpha_n x_1 - ({}_{1\mu_n} \cosh \beta_n x_1 + {}_{1\nu_n} \sinh \beta_n x_1) \sin \alpha_n x_1 \quad (44)$$

$${}_1O'_n(x_1) =$$

$$\left[\frac{i\tau_n}{EA_1} \sinh \beta_n x_1 + ({}_{1\delta_n} \beta_n - {}_{1\nu_n} \alpha_n) \cosh \beta_n x_1 \right] \sin \alpha_n x_1 +$$

$${}_1P'_n(x_1) = \left[\frac{i\sigma_n}{EA_1} \cosh \beta_n x_1 + ({}_{1\nu_n} \beta_n + {}_{1\delta_n} \alpha_n) \sinh \beta_n x_1 \right] \cos \alpha_n x_1 -$$

$${}_1O''_n(x_1) = \left[\frac{i\tau_n}{EA_1} \cosh \beta_n x_1 + ({}_{1\delta_n} \beta_n - {}_{1\nu_n} \alpha_n) \sinh \beta_n x_1 \right] \cos \alpha_n x_1 -$$

$${}_1P''_n(x_1) = \left[\frac{i\sigma_n}{EA_1} \sinh \beta_n x_1 + ({}_{1\nu_n} \beta_n + {}_{1\delta_n} \alpha_n) \cosh \beta_n x_1 \right] \sin \alpha_n x_1 \quad (45)$$

$$25 \text{ where } n=1, 2, \dots, n.$$

If the rod string is untapered, calculate the pump displacement and load from

$$30 u(x_1, t) = \frac{i\sigma_0 x_1}{2EA_1} + \frac{i\nu_0}{2} + \sum_{n=1}^{\bar{n}} {}_1O_n(x_1) \cos n\omega t + {}_1P_n(x_1) \sin n\omega t \quad (46)$$

$$F(x_1, t) =$$

$$35 EA_1 \left[\frac{i\sigma_0}{2EA_1} + \sum_{n=1}^{\bar{n}} {}_1O'_n(x_1) \cos n\omega t + {}_1P'_n(x_1) \sin n\omega t \right].$$

If the rod string is tapered, proceed to step 3.

Step 3. Calculate recursively the quantities

$${}_{j+1}\nu_o = \frac{j\sigma_0 x_j}{EA_j} + \nu_o$$

$${}_{j+1}\nu_n = {}_jO_n(x_j)$$

$${}_{j+1}\delta_n = {}_jP_n(x_j) \quad (44)$$

$${}_{j+1}\sigma_0 = \sigma_0$$

$${}_{j+1}\sigma_n = EA_j {}_jO'_n(x_j)$$

$${}_{j+1}\tau_n = EA_j {}_jP'_n(x_j)$$

$${}_{j+1}\kappa_n = \frac{{}_{j+1}\sigma_n \alpha_n + {}_{j+1}\tau_n \beta_n}{EA_{j+1} (\alpha_n^2 + \beta_n^2)} \quad (45)$$

$${}_{j+1}\mu_n = \frac{{}_{j+1}\sigma_n \beta_n + {}_{j+1}\tau_n \alpha_n}{EA_{j+1} (\alpha_n^2 + \beta_n^2)}$$

$$60 {}_{j+1}O_n(x_{j+1}) = ({}_{j+1\kappa_n} \cosh \beta_n x_{j+1} + {}_{j+1\delta_n} \sinh \beta_n x_{j+1}) \sin \alpha_n x_{j+1} + ({}_{j+1\mu_n} \sinh \beta_n x_{j+1} + {}_{j+1\nu_n} \cosh \beta_n x_{j+1}) \cos \alpha_n x_{j+1} \quad (46)$$

$$65 {}_{j+1}P_n(x_{j+1}) = ({}_{j+1\kappa_n} \sinh \beta_n x_{j+1} + {}_{j+1\delta_n} \cosh \beta_n x_{j+1}) \cos \alpha_n x_{j+1} - ({}_{j+1\mu_n} \cosh \beta_n x_{j+1} + {}_{j+1\nu_n} \sinh \beta_n x_{j+1}) \sin \alpha_n x_{j+1} \quad (47)$$

$$65 {}_{j+1}O'_n(x_{j+1}) = \left[\frac{{}_{j+1}\tau_n}{EA_{j+1}} \sinh \beta_n x_{j+1} + ({}_{j+1\delta_n} \beta_n - {}_{j+1\nu_n} \alpha_n) \cosh \beta_n x_{j+1} \right] \sin \alpha_n x_{j+1} +$$

$$70 {}_{j+1}P'_n(x_{j+1}) = \left[\frac{{}_{j+1}\sigma_n}{EA_{j+1}} \cosh \beta_n x_{j+1} + ({}_{j+1\nu_n} \beta_n + {}_{j+1\delta_n} \alpha_n) \sinh \beta_n x_{j+1} \right] \cos \alpha_n x_{j+1} +$$

$$75 {}_{j+1}O''_n(x_{j+1}) = \left[\frac{{}_{j+1}\tau_n}{EA_{j+1}} \cosh \beta_n x_{j+1} + ({}_{j+1\delta_n} \beta_n - {}_{j+1\nu_n} \alpha_n) \sinh \beta_n x_{j+1} \right] \cos \alpha_n x_{j+1} -$$

$$({}_{j+1\nu_n} \beta_n + {}_{j+1\delta_n} \alpha_n) \sinh \beta_n x_{j+1} \cos \alpha_n x_{j+1} \quad (48)$$

(47)

$$\begin{aligned} i+1P'_n(x_{i+1}) = & \left[\frac{i+1\tau_n}{EA_{i+1}} \cosh \beta_n x_{i+1} + \right. \\ & \left. (i+1\delta_n \beta_n - i+1\nu_n \alpha_n) \sinh \beta_n x_{i+1} \right] \cos \alpha_n x_{i+1} - \\ & \left[\frac{i+1\sigma_n}{EA_{i+1}} \sinh \beta_n x_{i+1} + \right. \\ & \left. (i+1\nu_n \beta_n + i+1\delta_n \alpha_n) \cosh \beta_n x_{i+1} \right] \sin \alpha_n x_{i+1} \end{aligned}$$

where $i=1, 2, \dots, m-1$, and $n=1, 2, \dots, \bar{n}$.

The pump displacement and load can then be calculated from

$$\begin{aligned} u(x_m, t) = & \frac{m\sigma_0}{2EA_m} x_m + \frac{m\nu_0}{2} \\ & + \sum_{n=1}^{\bar{n}} O_n(x_m) \cos n\omega t + P_n(x_m) \sin n\omega t \end{aligned} \quad (48)$$

$F(x_m, t) =$

$$EA_m \left[\frac{m\sigma_0}{2EA_m} + \sum_{n=1}^{\bar{n}} O'_n(x_m) \cos n\omega t + P'_n(x_m) \sin n\omega t \right]$$

Concisely stated, solutions to the equation

$$\frac{\partial^2 u(x, t)}{\partial t^2} = a^2 \frac{\partial^2 u(x, t)}{\partial x^2} - c \frac{\partial u(x, t)}{\partial t}$$

are obtained which, when evaluated at the surface, satisfy the measured conditions of the load-time curve and the displacement-time curve (charted on the recorder 35) represented by the equations

$$D(\omega t) = L(\omega t) - W_r = \frac{\sigma_0}{2} + \sum_{n=1}^{\bar{n}} \sigma_n \cos n\omega t + \tau \sin \omega t$$

and

$$U(\omega t) = \frac{\nu_0}{2} + \sum_{n=1}^{\bar{n}} \nu_n \cos n\omega t + \delta_n \sin n\omega t$$

respectively. These solutions can then be used to determine the load and displacement at any depth in the well, particularly at the pump, by using the basic diagnostic equations

$$F(x, t) = EA \left[\frac{\sigma_0}{2EA} + \sum_{n=1}^{\bar{n}} O'_n(x) \cos n\omega t + P'_n(x) \sin n\omega t \right] \quad (49)$$

and

$$U(x, t) = \frac{\sigma_0 x}{2EA} + \frac{\nu_0}{2} + \sum_{n=1}^{\bar{n}} O_n(x) \cos n\omega t + P_n(x) \sin n\omega t \quad (50)$$

The Equations 49 and 50 give force and displacement at arbitrary depth and can be used to calculate subsurface dynamometer cards such as the one shown in FIGURE 6.

The above equations 49 and 50 can be solved by programming a digital computer and then supplying the well test data in the proper form. For example, a standard digital computer can be programmed and the test data transcribed to punched cards or tapes. The test data can be transcribed by measuring the polished rod load in FIGURE 3 at various times to obtain a plurality of prints. Normally 60 or more points per complete cycle will provide sufficient points. A similar number of points are obtained for the polished rod displacement curve of FIGURE 4. In addition, a set of punched cards are prepared for the fixed data such as weight of polished rod, pump period, length of various rod segments and sizes and the unit weight of the various rod segments.

The exact program for the computer can be developed

by those skilled in the art and the exact form of the program will vary from worker to worker. The computer will supply a plurality of ordinate points that can be used to plot a dynamometer card for a selected depth. Normally the selected depth will be at the junction between two different sections of rod or at level of the pump.

An analog computer can also be used to provide a solution to Equations 49 and 50. An inspection of Equation 1 shows that it has the same form as the equation of an electrical transmission line

$$L \frac{\partial^2 Q}{\partial t^2} + R \frac{\partial Q}{\partial t} = \frac{1}{C} \frac{\partial^2 Q}{\partial x^2}$$

wherein L , R and C =inductance, resistance and capacitance, respectively, Q =charge in coulombs, x =distance in feet, and t =time in seconds. This equation can be simulated by the circuit of FIGURE 7 with magnitude of the capacitance, resistance and inductance being chosen to correspond to the features of the mechanical system.

The equivalent circuit of FIGURE 7 can be incorporated in a special analog computer or solved by a general purpose computer. A specialized computer is shown in block diagram form in FIGURE 8. The computer of FIGURE 8 can be connected directly to the load cells and displacement transducers shown in FIGURES 1 and 2. The computer will then supply a dynagraph card for any desired level in the system. The level of the dynagraph card can be selected by varying the current supplied to the equivalent transmission line shown in FIGURE 7.

The circuit of FIGURE 8 uses a recorder 40 to record the load and displacement signals generated by the transducers of FIGURES 1 and 2. The recorder can be a magnetic tape recorder with provisions for playing back the recorded signals at approximately 100 times the recording speed. It is preferred that the playback speed be greater to reduce the size of the equivalent transmission line of FIGURE 7 and improve the performance of the system. The recorder supplies the two signals to a signal generator 41 that adjusts the current flow to obtain the dynagraph for the desired level. The signal generator contains the necessary operational amplifiers to both shape the signals and sum the signals.

The transmission line 42 is shown in detail in FIGURE 7 and consists of resistance, inductance and capacitance. The exact size of the elements will depend upon the physical characteristics of the sucker rod string and its length. In practice it has been possible to design a single equivalent electrical circuit to accept the following range of values for a sucker rod string length of 2000 to 15,000 feet, a diameter of $\frac{1}{2}$ to 1 inch and up to 20 subdivisions.

The transmission line 42 is connected to the recorder 43 that includes an oscilloscope for displaying the developed signal. Of course, the recorder 43 also includes circuits for adjusting the signals and adding fixed constants such as the weight of the sucker rod string. The signal displayed on the oscilloscope will be in the form of a dynagraph card for the selected depth. The signal on the oscilloscope can be photographed to obtain a permanent record of the dynagraph card.

To demonstrate the type of information generated with this technique, the data shown in FIGURES 3 and 4 have been analyzed.

These data pertain to a well being produced with a 120-inch stroke unit pumping at 12 strokes per minute from a depth of 7500 feet. The rod string consists of 1425 feet of 1-inch rods, 1775 feet of $\frac{7}{8}$ -inch rods, and 4300 feet of $\frac{3}{4}$ -inch rods.

As indicated by the equations, the forces and displacements in the solution are given as functions of time.

When force is plotted versus displacement for a given time, dynagraph cards can be constructed for all positions in the sucker rod string, including the pump. FIGURE 6 shows a closed periphery pump dynagraph card constructed from the example data. Significant quantitative information can be obtained from this card, such as

differential fluid load, gross pump stroke, effective volumetric displacement, and volumetric efficiency. Moreover, in the event of system malfunction, the shape of the card is indicative of the nature of the trouble. The interpretation of pump dynagraph cards is well known to those skilled in the art and will not be discussed since it is not the subject of this invention.

The plotted subsurface cards can also be used to detect tubing leaks, detect defective tubing anchors, calculate intermediate rod stresses, detect gas separation problems, calculate pump intake pressure and detect leaky pumps, to name a few applications. Thus, it can be seen that considerable quantitative information can be gained by using the herein-described method to plot subsurface dynamometer cards.

I claim as my invention:

1. A method of determining the performance characteristics of a pumping well wherein a reciprocating pump is located below the fluid level of the well and has a piston therein with a sucker rod string extending upward to a polished rod which is connected to a reciprocating prime mover means at the top of the well, said method comprising:

- (a) measuring the area of each rod size in the sucker rod string, the combined length of the rods in the sucker rod string, the weight of the sucker rods and the pump, and the weight of that portion of the sucker rod hanging in said fluid;
- (b) actuating said sucker rod string to reciprocate the pump, whereby said pump piston generates acoustic waves which move along the sucker rod;
- (c) measuring and recording the load and displacement of the polished rod as functions of time;
- (d) selecting a depth within the well to be investigated and combining the corresponding components of the size and weight data measured in step (a) with the load and displacement versus time data measured in step (c) as the boundary conditions for a wave equation which describes the linear vibrations in a long slender rod, to determine the corresponding

forces and displacements in the sucker-rod stream at the selected depth; and

(e) plotting a curve of the load versus displacement for the selected depth.

5 2. A method of determining the performance characteristics of a pumping well as set forth in claim 1 wherein said curve is plotted for any desired depth level in the well by utilizing the relationships of load versus time and displacement versus time as expressed respectively by

10 the equations:

$$F(xt) = EA \left[\frac{\sigma_0}{2EA} + \sum_{n=1}^{\infty} O_n'(x) \cos n\omega t + P_n'(x) \sin n\omega t \right]$$

15 and

$$u(xt) = \frac{\sigma_0 x}{2EA} + \frac{v_0}{2} + \sum_{n=1}^{\infty} O_n(x) \cos n\omega t + P_n(x) \sin n\omega t.$$

3. The method of claim 1 wherein steps (d) and (e) 20 comprise selecting a depth within the well to be investigated and combining the corresponding components of the size and weight data measured in step (a) with the load and displacement versus time data measured in step (c) as the boundary conditions for a wave equation 25 which describes the liner vibrations in a long slender rod to determine the corresponding forces and displacements in the sucker rod string at the selected depth to obtain a plurality of coordinates of load versus displacement; and plotting the load versus displacement coordinates to obtain a dynagraph card for the selected depth.

References Cited

UNITED STATES PATENTS

35 2,107,151 2/1938 Higginson ----- 73—168 X
2,596,361 5/1952 Blancher ----- 73—151 X
2,741,915 4/1956 Renken et al. ----- 73—151 X

JAMES J. GILL, *Acting Primary Examiner.*

40 J. H. WILLIAMSON, *Assistant Examiner.*